Int J Thermophys (2008) 29:1094–1106
DOI 10.1007/s10765-008-0434-9

Development of a Multiband near-to-far Infrared Radiance COmparator (MIRCO)

J. Joly · P. Ridoux · J. Hameury · M. Lièvre · J.-R. Filtz

Published online: 23 April 2008

Abstract In recent years, there has been a growing demand to calibrate industrial blackbodies both at short wavelengths for lower temperatures and at long wavelengths for higher temperatures. User requests cover a very wide temperature range, from −20°C to 1,500°C in the infrared bands used by thermal cameras or as defined by specific applications (especially the 1–3 µm, 3–5 µm, and 8–12 µm bands). Therefore, LNE (Laboratoire National de Métrologie et d'Essais) has developed a radiance comparator with a mirror-based optical system, an associated set of interference filter wheels, a modular holder for several infrared detectors, and a lock-in amplifier. This setup is designed to be very versatile in terms of wavelength and temperature. Targeted performances have a thermal resolution better than 0.05°C, and a known and controlled size-of-source effect (SSE). A silicon detector and a visible-to-near infrared integrating sphere were used to assess the stray light inside the housing, and supplementary baffles and stops were used to reduce it to an acceptable level. The investigation included measurement of the SSE for this comparator layout. Then, the performance in the 3–5 µm and 8–12 µm bands, using, respectively, indium antimonide (InSb) and mercury cadmium telluride (MCT) detectors, was evaluated using a water heat-pipe blackbody. This paper describes the modeling and the technical solutions implemented to optimize the optical system. Preliminary results are presented for the short-term stability, the thermal resolution between −20°C and 960°C, and also the SSE up to 60 mm in these bands.

Keywords Blackbody · Calibration · Infrared · Multiband · Radiance comparator · Size-of-source effect

J. Joly (✉) · P. Ridoux · J. Hameury · M. Lièvre · J.-R. Filtz
CMSI 365, Laboratoire National de métrologie et d'essais, 29 Avenue Roger Hennequin, 78197 Trappes, France
e-mail: julien.joly@lne.fr

1 Introduction

Calibration of industrial blackbodies is part of the day-to-day activities of LNE. Many years ago, only users of thermal imaging systems, i.e., the defense sector, had needs in the 3–5 µm and 8–12 µm spectral bands between ambient temperature and 1,000°C. For a long time, we have been using commercial radiation thermometers or thermal cameras as optical comparators in conjunction with variable-temperature reference blackbodies.

Nowadays, industrial needs (energy, automotive, etc.) globally have overtaken the defense requirements, which have become more demanding in terms of wavelength and temperature, from 100°C in the 1–3 µm band or −20°C in the 3–5 µm band and up to 1,500°C in the 8–12 µm or 8–14 µm bands.

The low-temperature limit in the 1–3 µm and 3–5 µm bands is mainly determined by the low level of emitted radiation, but the 1,500–1,600°C high-temperature limit is due to technology. The construction of a very high-temperature furnace demands a complex apparatus including expensive or fragile products such as heating elements, thermal insulators, vacuum pumps, argon gas flow, and this results in untransportable equipment. Consequently, it is expected that the main calibration requests above 1,500°C will be for broadband spectroradiometers with infrared filters rather than blackbodies.

A few years ago, LNE decided to develop a Multiband near-to-far Infrared Radiance COmparator (MIRCO) with two applications in mind. The first one is to check the agreement among our own blackbody cavities by undertaking comparisons at specific wavelengths and in the thermal imagers' spectral bands. The second one is to extend our calibration capabilities for commercial blackbodies to lower temperatures and shorter wavelengths.

To be very versatile in terms of wavelength and temperature, this comparator was designed with the following specifications:

- broadband optical system: 0.8–14 µm
- temperature range from −20°C to 1,000°C in both the 3–5 µm and 8–12 µm bands
- a known and controlled size-of-source effect (SSE) to calculate a signal correction when comparing sources of different sizes
- good short-term stability (over the duration of the comparison)
- high thermal resolution to ensure a low contribution to the uncertainty budget

2 Design of the Multiband Infrared Radiance Comparator

2.1 General Presentation

To be able to use the comparator in a wide spectral range with a constant focal length, the optical system uses four aluminum-coated spherical mirrors (Fig. 1). Mirrors with focal lengths ranging from 250 mm to 800 mm are placed in small-footprint gimbal mounts; the system angular magnification is about 0.5. As suggested in [1], following Lyot's work, the aperture stop is placed after the field stop, in the plane of the last image of the first mirror. The resulting characteristics are a 400 mm working distance from

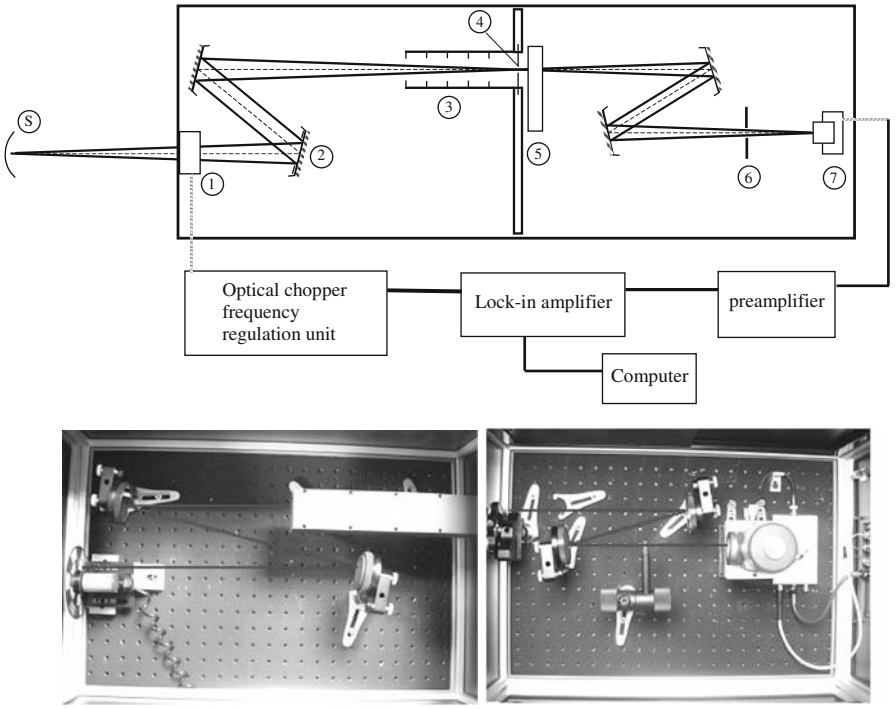

Fig. 1 Functional diagram of the near-to-far infrared comparator device; (S) source; (1) optical chopper; (2) mirror equipped with a limiting circular aperture; (3) baffle assembly; (4) field stop; (5) filter wheel; (6) aperture stop (pupil); (7) detector

the front flange, a f/8 numerical aperture determined from a ray tracing calculation, and a 3 mm geometrical target size.

Spectral selection is done by interference filters embedded in a mechanically indexed wheel for precise positioning when switching from one filter to another. Two filter holders are available, one for the classical bands (including 3–5 µm and 8–12 µm bands) and another to meet custom calibration requests. Because of the small angles (from 6° to 8°) needed to reduce optical aberrations, particular attention was paid to the stray light reduction within the collection part of the system. All the housing's internal walls are coated with 3M Nextel 811–21 paint to ensure a high absorbance from the visible to the far–infrared. A black-painted baffle assembly is placed close to the field stop to avoid direct rays from the source.

All the components are mounted on pedestal risers that can be clamped anywhere on an optical breadboard to ensure stability and flatness with maximal flexibility. The result is very good mechanical stability with the possibility to easily include additional elements for future applications. The measurement chain includes liquid-nitrogen (LN_2)-cooled quantum detectors (listed in Table 1) with associated preamplifiers, an optical chopper, and a lock-in amplifier. The use of an optical modulation system at the entrance port of MIRCO does not allow the radiation coming from the

Table 1 Summary of detectors used in MIRCO

Detector type	Purchase year	Manufacturer model	Preamplifier type	F.O.V.[a] (°)	Size of element[a] (mm)	D^{*}[a] @ λ peak (cm · $Hz^{1/2}$ · W^{-1})	λ Peak[a] (μm)	Window[a]
InSb	2006	Judson/ J10D-M204-R04M	PA-9	10	dia. 4	2.6×10^{11}	5.3	Sapphire
InSb	2002	Hamamatsu/ P7751-02	Built-in	60	dia. 2	2.0×10^{11}	5.3	Sapphire
MCT	2006	Judson/J15D 14-M204-S02M-	PA-300	10	2 × 2	6.4×10^{10}	12.5	ZnSe
MCT	2002	Hamamatsu/ P7752-10SPL	Built-in	60	2 × 2	3.0×10^{10}	15.0	ZnSe

[a] Manufacturer specifications

optical elements to contribute to the output signal, except for a negligible portion that would be modulated at the same frequency.

2.2 Near-Infrared Size-of-Source Effect Characterization

To evaluate the SSE of MIRCO in the near-infrared band, initial tests were performed with a Hamamatsu 1337 type silicon detector filtered at 900 nm and connected to a LNE-fabricated current-to-voltage amplifier. For this investigation, the optical chopper was removed and the signal measured with a nanovoltmeter.

The experimental setup (Fig. 2) is based on the direct method: the comparator is focussed at the center of a bright circular region whose diameter d can be changed by replacing the limiting diaphragm [2]. The source is a 100 mm exit port integrating sphere with an internal quartz halogen lamp supplied by a high-stability current (stable to 1×10^{-5}A). The variable aperture is implemented by combining several small stops (1–4 mm) with a steel iris diaphragm of 60 mm maximum aperture. Following [3], the variable aperture is decoupled from the exit port of the sphere in order to reduce radiance variations when changing the source diameter.

The SSE corresponding to any d value is calculated as the ratio of the signal obtained when d equals $d_{\max}$, after correcting for the background signal V_0:

$$\mathrm{SSE}(d; d_{\max}) = \frac{V_d - V_0}{V_{d\max} - V_0} \quad \text{with } d_{\max} = 60 \text{ mm} \tag{1}$$

The results presented in Fig. 3 are from five runs with 50 individual readings at each diameter. The uncertainty bars show the associated global standard deviation.

The results show a very low sensitivity to the radiance coming from the surroundings of the target area. The observed value of SSE(3;60) is 0.99971. This means that

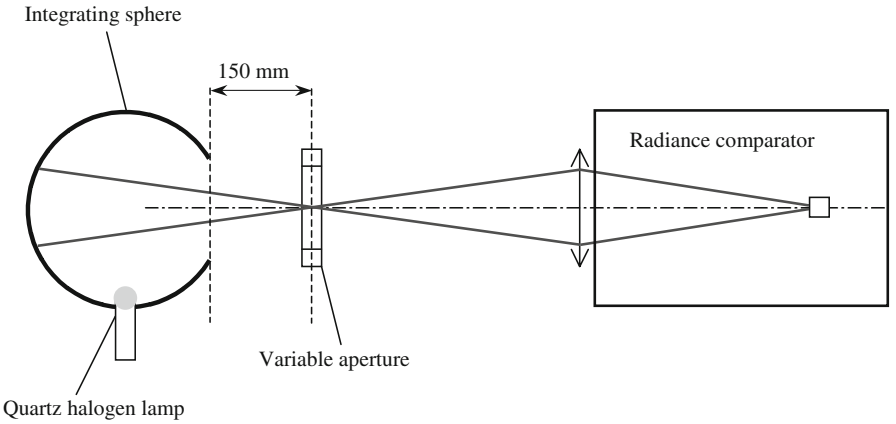

Fig. 2 Experimental setup for the SSE measurement in the visible and in the near-infrared

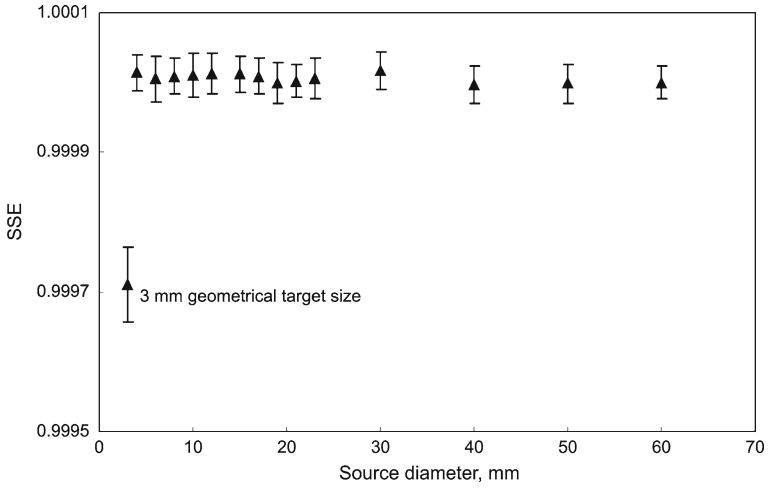

Fig. 3 SSE results for MIRCO filtered at 900 nm

the relative correction, ΔSSE, is less than 3×10^{-4} for a source of the same size as the geometrical target (3 mm);

$$\Delta\,\mathrm{SSE}(d) = 1 - \mathrm{SSE}(d, d_{\max}) \tag{2}$$

For source diameters larger than 4 mm, the corrections are smaller than the measurement dispersion, about 2.5×10^{-5} (1σ) on average.

In the near-infrared, the indirect method, with a central obscuration of the source, is currently used [4] instead of the direct method because of its better resolution. Nevertheless, the direct method was preferred for compatibility with the procedure implemented in the mid- and far-infrared (Sect. 3.3).

3 Characterization of Mid- and Far-Infrared Settings

As the demands for calibrating blackbodies are mainly in the mid- and far-infrared, MIRCO was studied for short-term stability, thermal resolution, and SSE, especially in the 3–5 µm and 8–12 µm bands. In this application, all detectors are underfilled; the image on the detector is about 1.5 mm diameter, and the smallest sensing element is a $2 \times 2\,\text{mm}^2$ chip. Detectors were purchased from Judson with a specific field of view adapted to the optical system.

3.1 Short-Term Stability

The short-term stability of MIRCO was estimated over a period corresponding to the time needed for the comparison of two sources. A comparison cycle is completed when the measurement of the blackbody under calibration is bracketed by two measurements on the reference blackbody. This requires approximatively 15 min, depending on the lock-in amplifier settings (time constant, number of readings).

The source used for this test is a KE Technology water heat-pipe blackbody (WHP BB) fitted with a Model 162 Rosemount standard platinum resistance thermometer (SPRT) close to the cavity back wall. The copper alloy cavity was coated with a specific black paint to ensure a high emissivity in the 3–15 µm spectral range. The spectral emissivity of this paint was measured at LNE [5].

The WHP BB stability at 200°C is typically better than 20 mK over a 2 h period (Fig. 4). According to [6], the stability is limited by the temperature feedback and by the PID control software of the heating elements.

MIRCO was tested with the Judson detectors in three configurations: Indium antimonide(InSb) detector plus 3–5 µm filter, mercury cadmium telluride (MCT) detector plus 3–5 µm filter, and MCT detector plus 8–12 µm filter.

In each case, the experimental procedure was as follows:

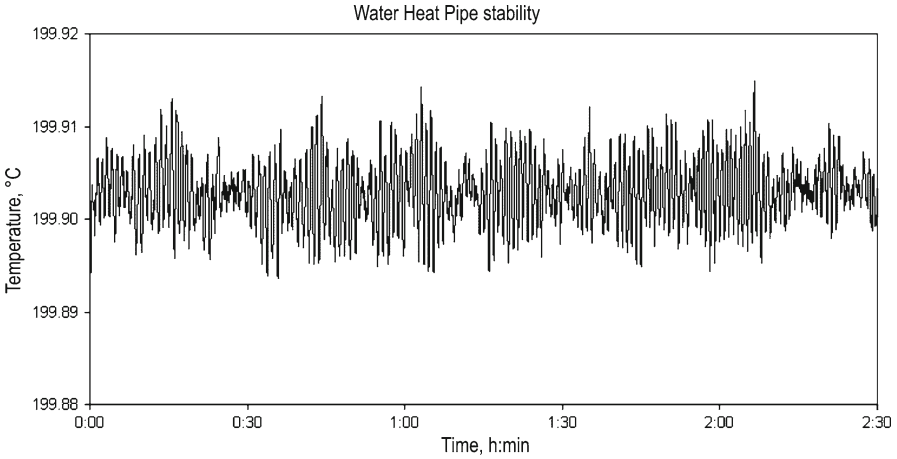

Fig. 4 Water heat-pipe blackbody stability measured with a SPRT close to the back wall of the cavity

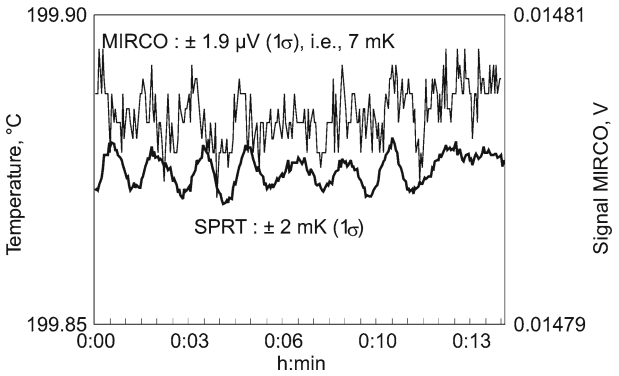

Fig. 5 Short-term stability for MIRCO with InSb/3–5 µm compared with the water heat-pipe blackbody temperature

– fill the LN_2 Dewar of the detector 30 min before starting measurements
– aim the MIRCO at a stable source at 200°C
– measure the SPRT resistance and detector voltage versus time for at least 15 min

The final results show a short-term stability better than 15 mK for each configuration of MIRCO. The values obtained with the InsSb detector are presented in Fig. 5.

3.2 Thermal Resolution (NETD)

The noise-equivalent temperature difference (NETD) is the temperature difference that produces a signal-to-noise ratio of unity [8]. It is evaluated by the following relation:

$$\mathrm{NETD} = \frac{Noise_{\mathrm{rms}}}{Se(T)} \tag{3}$$

where noise is defined as the rms deviation of the detector output from its average value and $Se(T)$ $(V \cdot {}^{\circ}\mathrm{C}^{-1})$ is the sensitivity of the instrument.

The sensitivity of MIRCO for each Judson-based configuration was determined from a calibration performed with several blackbodies. To prevent drift of the comparator, all calibrations were performed within a short time.

The NETD was determined from the zero-signal noise, evaluated with a blackbody source set at the apparent temperature of the optical chopper. A summary of the NETD calculated at different blackbody temperatures is listed in Table 2.

Some values seem to be very small, especially at high temperatures, but it must be mentioned that noise coming from a source at room temperature is very limited; no temperature fluctuations due to a heating or cooling process are observed, and the low heat transfer between room air and the cavity is advantageous (no convection). The thermal resolution of the instrument can be assessed without the influence of the radiating source.

Table 2 Summary of the NETD

Detector ref	Filter	@−20°C	@20°C	@80°C	@200°C	@600°C	@900°C
		(mK)					
J-InSb	3–5 µm	550	130	30	4	0.4	[a]
J-MCT	3–5 µm	2550	620	135	18	2	1
J-MCT	8–12 µm	34	20	13	8	4	4

[a] Out of range

3.3 Size-of-Source Effect (SSE)

3.3.1 Experimental Setup

A knowledge of the SSE is particularly critical for radiation thermometers in the far-infrared as it defines the limits of the equipment as a function of the geometry and radiance uniformity of the blackbody to be calibrated.

Preliminary investigations in the near-infrared (Sect. 2.2) have qualified the optical system over a spectral range where reliable and well-known facilities are currently used, such as a white-coated integrating sphere and a quartz halogen lamp. At longer wavelengths, a similar solution would be to use a gold-coated integrating sphere; however, difficulties such as non-uniformity due to the specular component of internal reflections and poor efficiency render the approach unsuitable. Therefore, the best facility available to measure the SSE in the 3–14 µm band is a large and uniform thermal source.

Consequently, a procedure equivalent to that for the near-infrared was used with the WHP BB to characterize MIRCO in the 3–5 µm and 8–12 µm bands. The aperture diameter of the cavity is 63 mm and can be varied from 10 mm to 60 mm with additional stops. The background signal was evaluated by aiming the comparator at the appropriate area of the smallest stop (Fig. 6). The stops are placed in a water-cooled holder and are thermally decoupled from the cavity to avoid disturbing the blackbody stability. This assumption was confirmed by monitoring the cavity temperature with an SPRT.

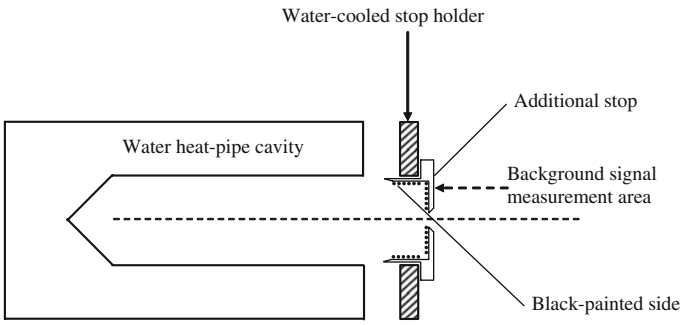

Fig. 6 Experimental setup for the SSE measurement in the far-infrared

Theoretically, the smaller the cavity aperture, the larger is the apparent emissivity. Each stop was blackened on the side facing the blackbody to reduce the radiance variation when measuring the SSE [7]. The apparent emissivity variations of this source were estimated using the software STEEP3^{TM} based on the Monte Carlo method. For this calculation, the source consists of an isothermal cavity at 200°C (WHP cavity) terminated with a stop at room temperature. The computation shows a maximum emissivity variation of less than 5×10^{-5} at 4 µm and less than 1×10^{-4} at 10 µm as the source aperture varies from 10 mm to 60 mm. No corrections were applied to the SSE values because of these low emissivity variations.

3.3.2 Results and Comments

As previously noted, Judson detectors are normally used with MIRCO. However, the temporary availability of other InSb/MCT type detectors from Hamamatsu provided an opportunity to evaluate the influence of some specifications, such as the size of the element and the field of view, on the SSE.

The following combinations of filters and detectors (size of element and field of view are listed in brackets) were studied:

- Judson_InSb (diameter 4 mm, FOV 10°) in the 3–5 µm band
- Hamamatsu_InSb (diameter 2 mm, FOV 60°) in the 3–5 µm band
- Judson_MCT ($2 \times 2\,mm^2$, FOV 10°) in the 3–5 µm and 8–12 µm bands
- Hamamatsu_MCT ($2 \times 2\,mm^2$, FOV 60°) in the 3–5 µm and 8–12 µm bands

The results are grouped by detector type for each spectral band: InSb/3-5, MCT/3-5, and MCT/8-12, respectively, in Figs. 7–9. Even if some comments below are explained in terms of Judson/Hamamatsu, the purpose is not to draw conclusions regarding the products of a particular manufacturer but to highlight the effects that arise from differences in geometrical parameters.

Some general conclusions can be drawn from these measurements. The SSE effect is somewhat higher for the Hamamatsu detectors; this may be due to the windows

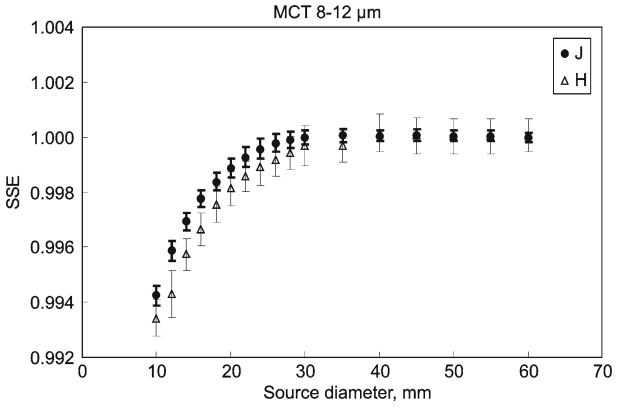

Fig. 7 SSE results for MIRCO with MCT/8–12 µm

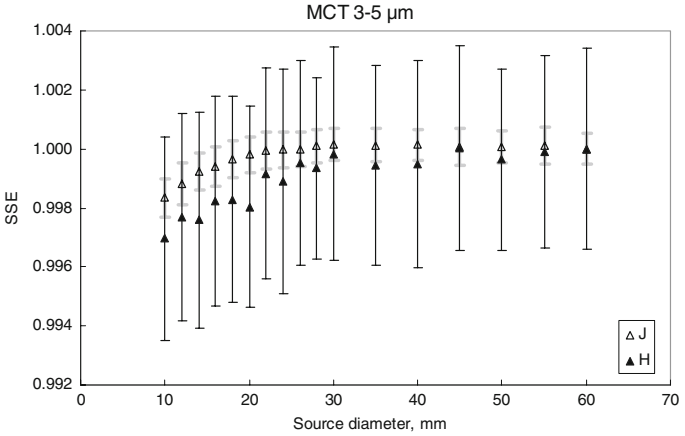

Fig. 8 SSE results for MIRCO with MCT/3–5 µm

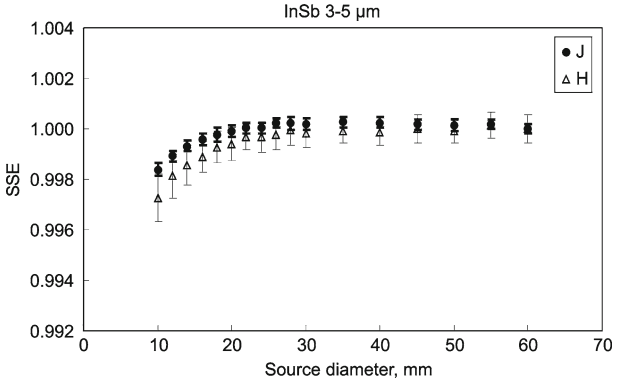

Fig. 9 SSE results for MIRCO with InSb/3–5 µm

being older and in worse condition or to a possible effect related to the cold shields. The dispersion of values is less important with the Judson detectors, probably because of their smaller field of view. Nevertheless, we are doubtful of the dispersion obtained with the Hamamatsu_MCT filtered in the 3–5 µm because erratic behavior was sometimes observed. No influence of the size of the sensing elements has been found for InSb detectors. The differences between the InSb and MCT detectors filtered in the same band (3–5 µm) are not significant for a given manufacturer. In fact, the spectral band is clearly the most influential parameter; the longer the wavelength, the larger is the SSE (Fig. 10). For example, a value of 3×10^{-4} for the SSE correction corresponds to a source diameter of 3 mm at 900 nm, 17 mm in the 3–5 µm band, and 25 mm in the 8–12 µm band. Another outcome is that the relative error in the radiance measurement when MIRCO is aimed at a source of 10 mm diameter is negligible at 900 nm but about 1.6×10^{-3} and 5.8×10^{-3}, respectively, for the 3–5 µm and 8–12 µm bands.

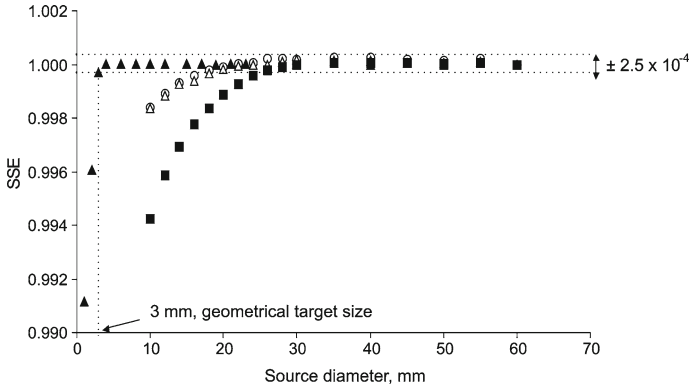

Fig. 10 Summary of SSE results for MIRCO from near-to-far infrared

The sensitivity of any radiance meter to the SSE can be converted to temperature using the derivative of Planck's law;

$$\frac{\Delta L}{L} = \frac{x}{1 - \mathrm{e}^{-x}} \frac{\Delta T}{T} \tag{4}$$

with $x = \frac{c_2}{\lambda T}$,

$$\text{then } \Delta T = \frac{\lambda T^2}{c_2}(1 - \mathrm{e}^{-x})\Delta\mathrm{SSE} \tag{5}$$

where L is the spectral radiance, T is the temperature, c_2 is the second radiation constant, and λ is the central wavelength of the radiance meter.

Table 3 lists some values of the SSE correction of 3×10^{-4}, expressed as temperature differences versus wavelength at different source temperatures.

3.4 Modeling the Size-of-Source Effect: First Investigations

The SSE has been recognized and assessed for a long time, and a comprehensive approach was published in 1997 [4]. As a complementary task to the experimental

Table 3 Corrections (mK) for an SSE value of 3×10^{-4} as a function of wavelength and temperature

Temperature (°C)	$\lambda = 0.9\,\mu\mathrm{m}$	$\lambda = 4\,\mu\mathrm{m}$	$\lambda = 10\,\mu\mathrm{m}$
	(mK)		
50	2	9	22
500	12	49	105
1,500	60	227	364
2,000	97	342	505
2,500	144	466	650

assessments described in Sects. 2.2 and 3.3, we wanted to check if the modeling approach, with its ability to consider a large number of otherwise unobtainable physical configurations, could help to pinpoint the main design features giving rise to the SSE.

The measurements have demonstrated the dependence of the SSE on wavelength. We take as an indicator the size range in which the signal increases from 0 to (1σ) of the extrapolated stabilized value, where σ is the repeatability component of the measurement uncertainty. This indicator increases from around 3.5 mm at 900 nm to 26 mm in the 8–12 µm band, and is 18 mm in the 3–5 µm band. The possible effects behind this behavior include scattering from optical surfaces, scattering from particles in the air, diffraction by apertures, and aberrations. Usually, with longer wavelengths, scattering processes become less intense but more directive, diffraction effects increase, and aberration effects tend to decrease. All these effects combine to generate the wavelength dependence, and the resulting dependence varies significantly with the optical design.

This was an opportunity to assess the capabilities of a specific optical modeling tool. In the future, this tool may be used to enhance similar optical designs at an early stage. These investigations depend strongly on the software, which is Zemax™ in our case. The user can easily create optical surfaces and objects and import parts from other drawing tools. As far as stray light is concerned, the application is preferably run in the non-sequential mode, which allows rays to be traced from any prescribed surface to any other one, including multiple reflections. After appropriate learning, the user can apply accurate wavelength-dependent surface properties and use the integrated programming language to explore the effects of different parameters.

The pitfall of such an approach is that it is very time consuming: the expected effects have a magnitude of a few tens of ppb (part per billion), which implies launching at least 100,000 rays. If multiplied by the number of parameter values, the computation time is easily several hours using a fast but affordable desktop computer. Eventually, it becomes quite impractical to quickly assess the global response to a variable-size source. As a possible way to get around such limitations, we were able to program a point source moving from the center to the edge of the actual source, emitting rays only toward the entrance port, and thereby enhancing the launching efficiency of rays from 38 ppb to 1 (the angular aperture of the entrance port is 0.5°). We can consider a few parameters independently, mainly the scattering from optical surfaces and diffraction from the mirror and stop edges; these can be specified as wavelength-dependent.

Another pitfall lies in the difficulty in giving realistic values to the scattering properties. Lambertian scattering is the most likely for non-optical surfaces, but is also less efficient for ray tracing. If this broad scattering function is replaced with a Gaussian one with a small but arbitrary angle about the specular direction, the efficiency is enhanced at the expense of losing the overall quantification: there is no simple way to reverse the process and compute how many rays would have hit the detector without the Gaussian hypothesis.

However, Zemax™ has proved rather reliable for the aberration effect, as expected from such a ray tracing application. It accounts for the first few millimeters of the SSE, validating the optical design. Diffraction is expected to cause the main part of the wavelength variability. The possibilities are yet to be investigated, but we intend to proceed in this direction by taking into account all the know-how gained at this early stage.

4 Conclusion and Prospects

LNE has developed a multiband near-to-far infrared radiance comparator MIRCO to strengthen its measurement facilities in radiation thermometry with an instrument that is versatile in terms of wavelength and temperature.

The characterization of the instrument was first performed at low temperature in the 3–5 µm and 8–12 µm spectral bands, typical of customers needs. The short-term stability and thermal resolution have been studied. Particular attention was paid to the SSE, which is of great importance when comparing two sources. The influence of wavelength on the SSE was highlighted by using various Si, InSb, and MCT detectors with the same mirror-based optical system.

Supplementary investigations are planned to achieve a thorough characterization. In the near-infrared, the low SSE observed with the direct method requires a more sensitive method (indirect) to be implemented. The spectral analysis will be completed with additional bandpass filters (1–3 µm, 3.7–5.2 µm, 8–14 µm) and detectors (extended InGaAs, pyroelectric). A continuously variable spectral filter can be easily inserted into the optical path.

Some complementary measurements must be performed with a fixed-point blackbody to study the stability and the repeatability (influence of the thermal radiation from the chopper). Further improvement will consist of adding a variable-temperature source seen by a mirror blade optical chopper to overcome the measurement limitation around room temperature. Numerical modeling is still at an early stage. It is expected to give deeper insight into understanding the main design features giving rise to the SSE and hopefully will offer suggestions regarding how to reduce it further.

Acknowledgment Authors sincerely thank Thierry Valin for his helpful work on the data acquisition software.

References

1. H. Yoon, D.W. Allen, R.D. Saunders, Metrologia **42**, 89 (2005)
2. P. Bloembergen, Note on the size of source effect. *Final report TRIRAT Appendix E to the protocol*, SMT4-CT96-2060, pp. 95–96 (2001)
3. R. Winkler, E.R. Woolliams, W.S. Hartree, S.G.R. Salim, N.P. Fox, J.R. Mountford, M. White, S.R. Montgomery, in *Proceedings of TEMPMEKO* 2007, Int. J. Thermophys. **28**, 2087 (2007). doi: 10.1007/s10765-007-0275-y
4. P. Bloembergen, Y. Duan, R. Bosma, Z. Yuan, in *Proceedings of TEMPMEKO '96, 6th International Symposium on Temperature and Thermal Measurements in Industry and Science*, ed. by P. Marcarino (Levrotto and Bella, Torino, 1997), pp. 261–266
5. J. Hameury, B. Hay, J.R. Filtz, Int. J. Thermophys. **26**, 1973 (2005)
6. M. Noorma, S. Mekhontsev, V. Kromchenko, M. Litorja, C. Cagran, J. Zeng, L. Hanssen, Water heat pipe blackbody as a reference spectral radiance source between 50°C and 250°C. Thermosense XXVIII, Proc. of SPIE **6205**, 620502–620511 (2006)
7. Y. Kaneko, Y. Shimizu, J. Ishii, Numerical estimation of effective emissivities of low temperature blackbody cavities with apertures. SICE Annual Conference in Sapporo PR0002/04/0000, 1764–1767 (2004)
8. J.D. Vincent, *Fundamentals of Infrared Detector Operation and Testing* (Wiley-Interscience, New York, 1990)